Pure Appl. Chem., Vol. 78, No. 12, pp. 2205–2226, 2006.
doi:10.1351/pac200678122205

Laser nanochemistry*

Hiroshi Masuhara‡, Tsuyoshi Asahi, and Yoichiroh Hosokawa

Department of Applied Physics, Osaka University, Suita 565-0871, Japan

Abstract: Various time- and space-resolved spectroscopies have been developed and applied to thin films and nanoparticles. Dynamic reflection spectroscopies of total internal, diffuse, and regular reflection modes analyze photophysical and photochemical processes at the interface/surface layers with thicknesses of a few tens to a few hundreds of nm and of optically scattering materials. The excited singlet, triplet, and ionic states are identified, and intersystem crossing, isomerization, electron transfer and recombination, and photothermal conversion due to excited-state annihilation are analyzed, just as by transmittance mode spectroscopy. Fluorescence and Rayleigh light-scattering spectroscopies are developed for elucidating excited-state dynamics of single nanoparticles. The optical properties are related to their size, shape, internal structure, and environmental conditions. We prove that organic molecular materials show novel nanometer-size effects due to structural confinement. The high-intensity laser excitation induces ablation whose dynamics and mechanism are considered on the basis of time-resolved spectroscopy and imaging. For nanosecond and femtosecond ablation, we propose cyclic multiphotonic absorption and photomechanical mechanisms, respectively, while purely photochemical ablation was confirmed. Ablation studies have opened a new research approach toward expansion and contraction dynamics of polymer films, nanoparticle preparation, crystal growth control, crystallization in saturated solution, and others.

Keywords: time-resolved spectroscopy; reflection spectroscopy; microspectroscopy; laser ablation; nanoparticles; Porter Medal.

INTRODUCTION

Since the invention of the laser in 1960, it has been contributing greatly to the development of modern chemistry. Lasers were introduced very early in molecular spectroscopy and photochemistry studies, and have been used as light sources for spectroscopic measurements as well as for inducing photochemical reactions. Fundamental studies started with isolated molecules in the gas phase and in dilute solution, then shifted to more complex molecules, molecular aggregates, polymers, and have subsequently been extended to colloids and molecular solids. In addition, the development of photochemistry from homogeneous to inhomogeneous systems has led to the combination of lasers with optical microscopes [1–4]. Time-resolved spectroscopy has been extended to time- and space-resolved spectroscopy, while picosecond and femtosecond laser pulses have improved temporal resolution. Such utilization of ultrashort lasers and microscopes brought about the experimental conditions of high-intensity excitation, and consequently, laser ablation has gradually become familiar to photochemists. Intense irradiation of a laser pulse to molecular materials etches surface layers and small spots, which is now accepted

*Paper based on the acceptance lecture for a 2006 Porter Medal, presented at the XXI[st] IUPAC Symposium on Photochemistry, 2–7 April 2006, Kyoto, Japan. Other presentations are published in this issue, pp. 2193–2359.

‡Corresponding author

as a conventional fabrication method. The dynamics and mechanistic studies on ablation are scientifically important as they are expected to elucidate how electronic excitation of molecular materials evolves to their morphology changes. Thus, photochemistry using lasers in a small space is indeed innovative and is being recognized as laser nanochemistry. The main topics on which we have worked in the past quarter century are spectroscopy, photochemistry, and ablation [5–7], whose backgrounds are summarized as follows.

As a monochromatic light source, laser enables us to measure fine and precise spectra of molecules and to assign stable, excited, and transient molecular species; high-resolution spectroscopy. Moreover, very specific reactions can be controlled by using a small difference in electronic energy levels, whose representative example is laser isotope separation. Another contribution of the laser is surely a high potential in developing time-resolved spectroscopy. It is well known that M. Eigen, R. G. W. Norrish, and G. Porter were awarded the 1967 Nobel Prize for their work on fast reactions [8]. Their pump–probe experiments showed us how to interrogate dynamic chemical reactions. In the flash photolysis by Norrish and Porter, molecular excited states were produced by the irradiation of an intense flash lamp, and then the succeeding radicals, ions, isomers, and/or unstable intermediates were spectroscopically detected by a probing flash lamp. This pump–probe approach is now a standard in the analysis of chemical reactions and has been introduced widely into various spectroscopies. Norrish and Porter demonstrated it for UV–vis electronic absorption spectroscopy, whereas the approach now covers wavelength regions from X-ray to THz, and time regions from attoseconds to hours. Before the laser was invented, flash lamps were the only light source for absorption spectroscopy and their pulse width was limited to the microsecond. This is ascribed to the mechanism of electric discharge in gas tubes, and a new light source with a shorter pulse width was realized by introducing lasers. The first laser oscillation was achieved using a ruby laser, and its pulse duration was 10 ns. Later on, the improvement of pulse width reduced to a picosecond in the late 1960s, to sub-picoseconds in the middle of the 1970s, until the femtosecond laser was introduced in the early 1980s. These developments were so fast that novel chemistry achieved by such short laser pulses enjoyed rapid development, which is symbolized by the award of the 1999 Nobel Prize to A. H. Zewail [9], for advances in femtochemistry.

When spectroscopists and photochemists started to use pulsed lasers, they became aware that intense laser irradiation induced vaporization, decomposition, and fragmentation of materials, and found that the irradiated surface was etched. The residual pattern was used to confirm how a pulsed laser beam propagates on the optical table for spectroscopic experiments. This laser ablation phenomenon was soon utilized to fabricate microstructures of various materials, particularly by electronics engineers who paid much attention to the technique for future electronic device production, and by medical doctors who applied ablation to microsurgery. Application of this laser ablation to organic materials was started in the early 1980s [10], followed by subsequent studies on dynamics and molecular mechanisms. Again, the pump–probe approach was demonstrated to be suitable for elucidating the dynamics and for considering the evolution of molecular excitation energy in relation to ablation. Not only spectroscopic measurements, but also imaging methods for probing surface condition and fragmentation under ablation conditions, have been developed and applied to material fabrication. It is now recognized that it is both interesting and important to monitor how electronic excitation of molecules in a solid evolves into morphology changes, since this offers scope for development of various kinds of new tools, methods, and technologies based on laser ablation. The resultant chemistry is expanding contemporary research horizons in areas such as protein crystallization, growth control of crystals, patterning of protein cubes, and even manipulation of living cells in solution.

TIME- AND SPACE-RESOLVED SPECTROSCOPY AND PHOTOCHEMISTRY OF ORGANIC NANOMATERIALS

Traditionally, the target molecular systems to which pump–probe approaches have been applied are homogeneous systems of gas phase and dilute solution. Under transparent optical conditions, precise

transient absorption spectral measurement and detailed analysis of reaction kinetics can be performed, allowing correct assignment and straightforward understanding of reaction dynamics. In the studies on homogeneous systems, spectroscopic and dynamic data are due to an average of molecules that are in principle under the same conditions. However, once we shift our eyes to inhomogeneous systems and apply time-resolved spectroscopic methods, we have to solve many technical and analytical problems. Besides, the pump–probe approach for inhomogeneous systems was not popular and was initially not scientifically well founded. In the early 1980s [11], we started to improve time resolution of some reflection spectroscopies and applied them to nanomaterials such as small powders and crystals, thin films of nanometer thickness, and others.

A more direct approach to inhomogeneous molecular systems is to combine lasers with microscopes and to establish time- and space-resolved spectroscopic methods. This allowed us to measure small volumes in materials. Practically, we have conducted series of experiments on individual nanoparticles and assessed their electronic spectra, relaxation dynamics, and chemical reactivity as functions of size, shape, environment, internal structure, and other parameters. Furthermore, systematic studies of nanoparticles are very helpful to bridge our understanding of molecules and bulk materials.

Picosecond total internal reflection fluorescence spectroscopy

The internal reflection phenomenon is observed at the interface between two materials with different refractive indices. When light is introduced from the higher refractive index material to a lower index material, it is completely reflected at the interface under the condition that the incident angle is larger than a certain value. This angle is named the critical angle, for example, 58.7° for the air–toluene interface. At a larger incident angle than the critical one, light is reflected but it penetrates to some extent into the material with lower refractive index, which is called an evanescent wave. If this evanescent wave is used for fluorescence spectroscopy, molecules and materials at the interface layers where it can penetrate can be excited and detected. By changing the incident angle and/or excitation wavelength, we can probe the interface layer with different thickness. For air–solution and air–polymer combinations, the penetration depth of the evanescent wave is from a few tens to a few hundreds of nm. Although this internal reflection fluorescence spectroscopy was already in use before we started our experiments, no report had yet been presented on a time-resolved version. We succeeded for the first time in measuring fluorescence dynamics at the interface/surface layers by combining picosecond fluorescence spectroscopy based on single photon counting with the total internal reflection condition. This fluorescence spectroscopy has picosecond time and a few tens of μm space resolutions.

One of our systematic studies was on the interface layers of polymer solution-glass and polymer film-glass substrates. Fluorescence rise and decay kinetics show the different properties between the interface layer and bulk more sensitively than spectral shape. If the geometrical and electronic structures of molecules and of molecular aggregates and their distributions at the interface layer are different from those of the bulk, fluorescence peak wavelengths and spectral widths should be different from each other. Usually this is not probable, as electronic interactions of fluorescent molecules with surrounding solvent molecules and intermolecular interactions are weak. Specifically, the electronic energy difference, ΔE, between the layer and the bulk is small. However, the relaxation dynamics are considered to be more sensitive to ΔE, for example, the first order decay kinetics are proportional to $\exp(-\Delta E/kT)$. By using time-resolved total internal fluorescence spectroscopy of probe molecules in polymer solutions and films, we revealed various kinds of gradient from the interface to bulk in the depth region of a few tens and a few hundreds of nm for local structure of polymer films such as orientation of polymer side chains (substituents), polymer conformation, concentration of fluorescent probe molecules, and so on [11–26].

Nanosecond attenuated total internal reflection absorption spectroscopy

Pump–probe absorption spectroscopy was combined with a total internal reflection condition to measure transient absorption of the interface/surface layers. The excitation nanosecond pulse irradiated a sample polymer film on the quartz substrate from the perpendicular direction, and the monitoring probe light from a flash lamp was introduced to the quartz substrate and led to the polymer film under total internal reflection condition. The probe light then penetrates into the films as an evanescent wave, and the transient absorption is monitored. The thickness of the interface layers is dependent upon the incident angle and wavelength as described above. This spectroscopy was first demonstrated for a model system where a surface film with anthracene and a bulk film with benzophenone were layered [27], as shown in Fig. 1. The well-known triplet–triplet absorption spectra of the doped molecules is detected, and its relative contribution was changed with the incident angle as given in Fig. 2. The results indicate that the absorption spectra can be followed as a function of decay time with different thickness of interface and photophysical and photochemical dynamics in a few tens of nm interface can be clarified.

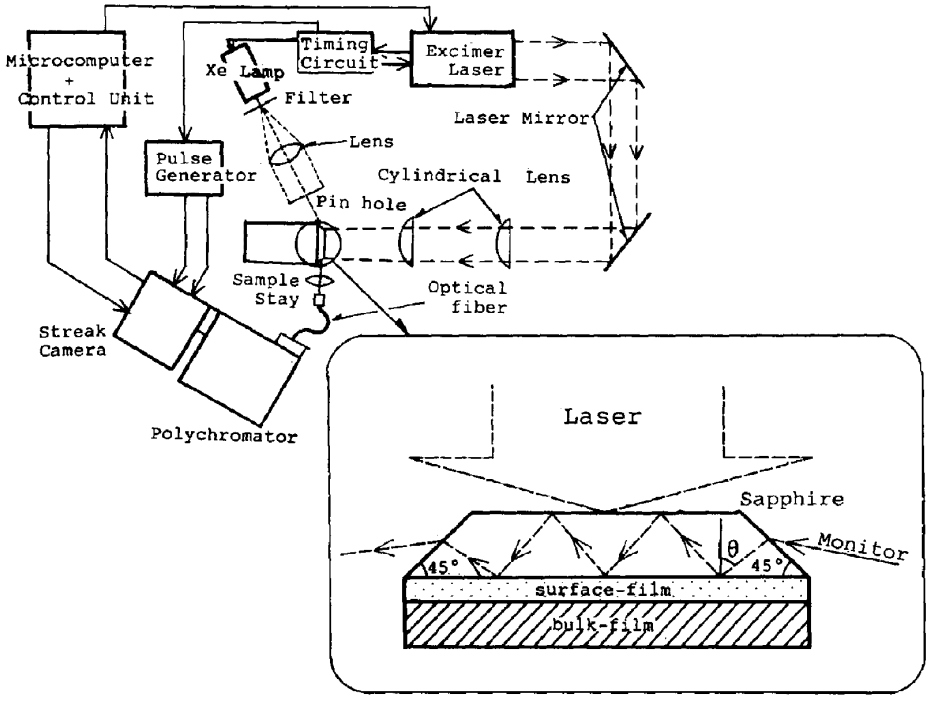

Fig. 1 Schematic diagram of a microcomputer-controlled system for nanosecond attenuated total reflection (ATR) UV–vis absorption spectroscopy. The inserted figure is an optical set of the sample where a bilayer model system consists of a thin surface film and a thick bulk film [27].

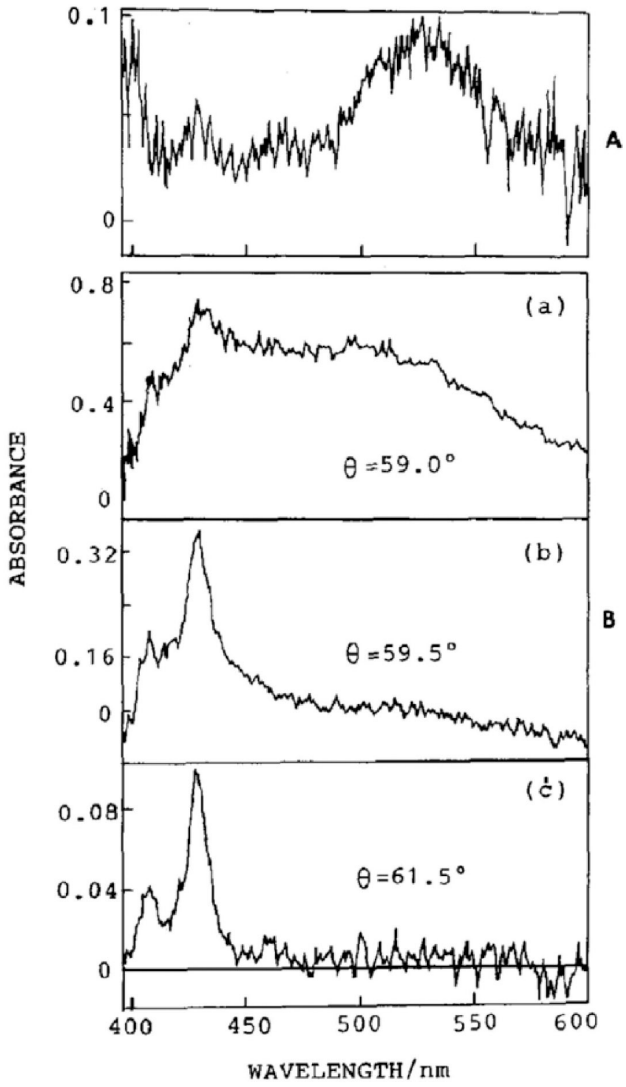

Fig. 2 Transient UV–vis absorption spectra of a model bilayer system; a surface film with a thickness of 240 nm and is doped with 2 wt % anthracene; the bulk film with a thickness of 200 μm and is doped with 15 wt % benzophenone. The delay time was 1 μm, and the gate width was 167 ns by the conventional transmittance method (A) and attenuated total internal reflection method (B). The incident angle is given in the figure [55].

Picosecond and femtosecond diffuse reflection spectroscopy

The first trial to introduce the pump–probe approach to optically scattering powders was done in 1981 by Wilkinson et al. [28], who proposed nanosecond diffuse reflection spectroscopy. Various kinds of powders as well as particles became research targets for transient absorption spectroscopy so that their excited singlet and triplet states, and neutral and ion radicals could be measured. Studies on organic microcrystals, photocatalytic semiconductor particles, zeolites, polymer particles, papers, textile fibers, and many scattering materials by time-resolved absorption spectroscopy were started, and their reported spectroscopic data indicate characteristic relaxation dynamics and chemical reactions [29–68].

Being stimulated by Wilkinson's works, we started to improve its time resolution up to the picosecond and femtosecond level, as we had understood the future potential of reflection spectroscopy by

developing time-resolved internal reflection spectroscopy. In 1987 and 1996 we reported the first papers on picosecond and femtosecond diffuse reflection spectroscopy, respectively [30,44]. In the picosecond system, the excitation pulse was about 20 ps, so that the broadening of pump and probe pulses during their propagation in the scattering samples were not distinct, but in the case of femtosecond spectroscopy, this broadening is indeed an important problem. This is clearly shown in Fig. 3, where the rise curve started from minus delay of a few tens of ps [55]. This seemed very strange when we observed this result for the first time. In the case of transparent samples, the pump and probe pulses propagate through a sample in the same direction and their relative speed is almost common. Generally, the origin of the time axis is defined as the time when both pulses arrive at the sample surface at the same time, so that the rise curve of the excited singlet state is usually sharp, corresponding to the convolution of both pulses. The fact that we could detect the absorption even at such minus delay time means that the probe pulse undergoes repeatedly reflection, refraction, and transmission and still remains in the sample when the excitation pulse comes to the sample later on.

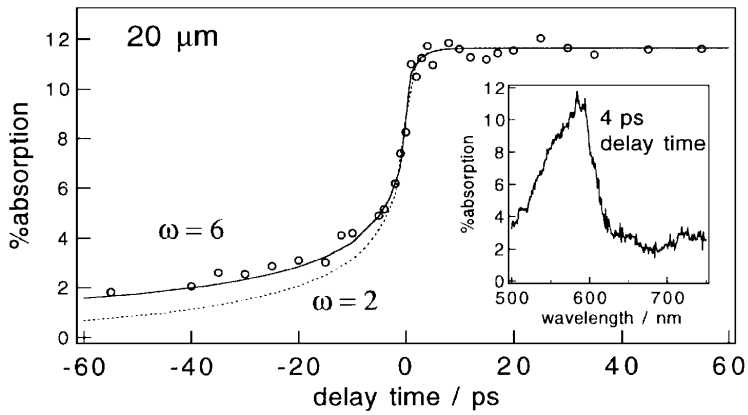

Fig. 3 Experimental and simulated rise curves of singlet excited-state absorption of 9,10-diphenylanthracene doped in PMMA powders. The parameter ω (2 and 6) means the diffuse light migrates longer than the straight path length by 2 and 6, respectively [55].

In the diffuse reflection spectroscopy, the parameter ω, representing how long the effective path length is in the scattering sample compared to transparent ones, is important. In steady-state and nanosecond diffuse reflection spectroscopy, ω is usually assumed to be equal to 2, which explains the experimental results. However, in our femtosecond diffuse reflection spectroscopy, ω is directly examined and we have come to the conclusion that ω is equal to 6 [55]. This means the light pulse propagates and remains for longer time than estimated and believed. The value of $\omega = 2$ is based on the model which is applied in the Kubelka–Munk theory, which assumes that a scattering sample consists of infinite numbers of thin layers, vertically incident light is being reflected or transmitted at each interface. The propagation along one direction was managed, but since actual systems involve reflection and refraction to all directions, then the effective path length represented by ω should be larger than 2. Now we can say that temporal correlation of two pulses propagating in scattering materials is obtained by measuring the excited singlet state of the anthracene derivative.

Representative absorption spectra, obtained by femtosecond diffuse reflection spectroscopy on microcrystalline spironaphthooxazine, are given in Fig. 4. Usually, it is difficult to prepare single crystals of suitable size for transmittance mode absorption spectroscopy, and the development of diffuse reflection spectroscopy was needed. This molecule isomerizes in solution and in polymer film, giving colored forms, but it is impossible in crystalline state as isomerization involves conformational change. One issue we could solve by our femtosecond system is the clarification of its primary processes in

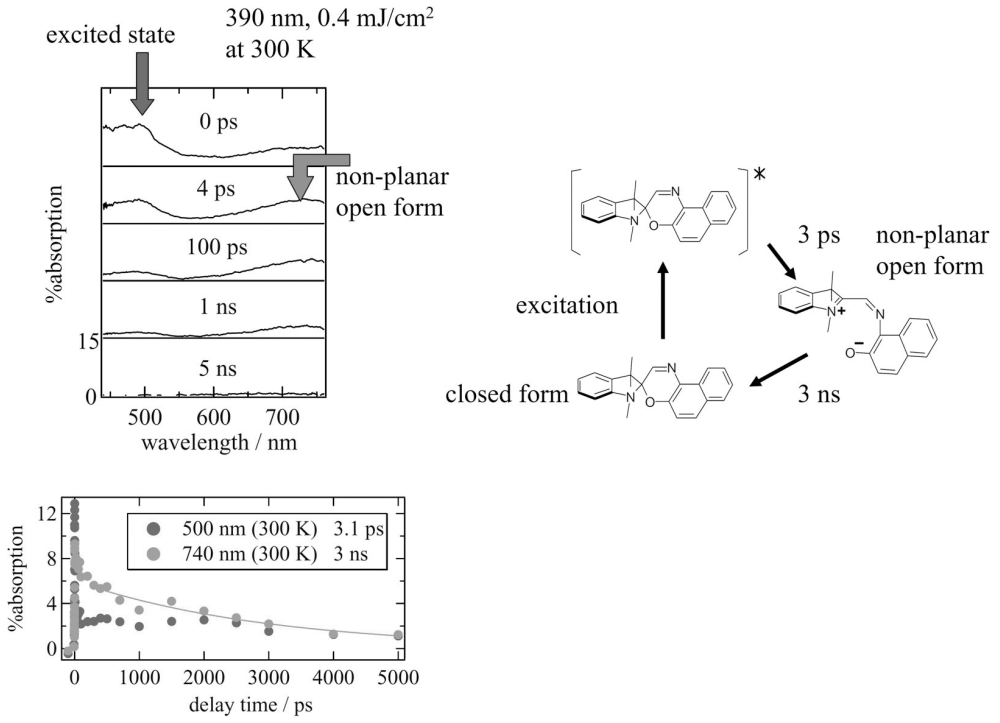

Fig. 4 Time-resolved diffuse reflectance spectra and dynamics of spironaphthooxazine microcrystals irradiated with 390 nm fs pulse at 0.4 mJ cm^{-2}.

multicrystalline solids. As shown in the figure, the excited state decays in a few ps and the transient absorption due to a nonplanar open form was detected later. However, no absorption remained after a few ns, indicating that the nonplanar open form comes back to the ground state of the starting molecule. Evidently, isomerization does not take place in the crystal as the conformational change involving the rotation is prohibited. It is worth noting that the quality of transient absorption spectra is at the same level as those of transparent solution systems, on which we can discuss ultrafast intersystem crossing, charge separation, exciplex formation, and photothermal heating processes characteristic of the "solid" state. The samples we have measured are micro/nanocrystals of aromatic molecules, dyes, EDA complexes, TiO_2, and also some polymer powders [29–68].

Picosecond and femtosecond regular reflection spectroscopy

The pump and probe approach was again combined with regular reflection spectroscopy, which makes it possible to measure excitation dynamics of organic materials having mirror-like surfaces. In our case, dye pellets were prepared and measured by exciting the surface layer with ultrashort laser pulses. The thickness of the exited and probed thin layers is a few tens of nm where both pump and probe pulses penetrate under the regular reflection condition. Spectral analysis is in principle the same as the conventional steady-state measurement, namely, the specular reflection spectra should be measured at different angles so that the laser-induced spectral changes of refractive index and extinction coefficient could be obtained. We have measured phthalocyanine pellets and clarified their exciton dynamics, their relaxation to hot ground states (vibrationally excited states in electronically ground states), and charge separation and recombination processes at the pellet/water interface [69–74].

One of the interesting results on dye samples in powders, films, and pellets, which are revealed by our time-resolved absorption spectroscopies described here, is their efficient photothermal conversion due to exciton-exciton annihilation leading to the ground state with excess vibrational energy [69,70,72–75]. The conversion process is the key to understanding why dye pigments are stable toward intense laser irradiation.

Femtosecond grating spectroscopy

In general, transient absorption of transparent films is measured by transmittance mode spectroscopy, while in the case of very thin films, the short path length is the main limitation to get enough data of quality with good signal-to-noise ratio. For nanometer thin films, it is usually not easy, but the problem is overcome by transient grating spectroscopy which we proposed in 1992 [76]. In the transient grating technique, two laser pulses of the same frequency are crossed in the film to generate optical interference patterns. A formed pattern of the excited states, ionic species, and refractive indices diffracts a probe pulse. Excitation energy transport in solids and solutions, carrier dynamics in semiconductors, orientational relaxation of molecular liquids, and related processes were studied, but they were usually probed only at a certain wavelength by using a monochromatic laser pulse. This means that excited species as well as transients are assumed in advance and their dynamics are then considered. However, photochemistry assumes that new reactions giving new spectra might be induced, and hence we always acquire absorption spectra. From this viewpoint, we introduce white light generated by focusing ultrashort laser pulse in water as a probe pulse and measure the pulse-induced diffraction spectra at different delay times. The diffraction measurement resembles a luminescent one, and it is not necessary to compare the diffracted signal to the incident light as in transmittance measurement. This means that the sensitivity is very high and the dynamic range is wide. Thus, we succeeded in getting absorption spectra of singlet and triplet states of benzophenone in solution [76] and excitation dynamics of phthalocyanine thin films [77]. It was successfully demonstrated that absorption spectra and their rise and decay kinetics can be followed even for thin film of a few tens of nm.

Picosecond-subμm fluorescence spectroscopy of single trapped microparticles

The time-resolved fluorescence spectroscopy under a microscope has been used widely in various fields, while our advantage is to apply this spectroscopy for laser-trapped single microparticles [1–3,78]. Particles and droplets undergoing micro-Brownian motion were individually trapped in solution by the photon force of a focused near-infrared laser beam and excited by picosecond or femtosecond laser pulses. The induced fluorescence is followed by single photon counting method and processed in a conventional way, which we achieved in 1991.

Femtosecond-μm absorption spectroscopy of single microparticles

The photophysical dynamics of nonfluorescent microcrystals was studied by developing femtosecond absorption spectroscopy under a microscope, and extended for measuring femtosecond spectra of single laser-trapped microparticles in solution in 1993 [79–81]. The pump and probe approach is now integrated to versatile time- and space-resolved spectroscopy, probing absorption and fluorescence, and converse various thin nanometer films and micro/nanoparticles.

Fluorescence and Rayleigh light-scattering spectroscopy and atomic force microscopy (AFM) observation of single nanoparticles

Fluorescence measurement itself has a high sensitivity, and even single-molecule detection becomes easy, so that fluorescence spectroscopy of single nanoparticles should not be difficult. The subject of

this spectroscopy is how to correlate spectroscopic data to shape, size, environment, and internal structure of the single particle. This was made possible by developing an integrated system shown in Fig. 5, where an AFM is equipped on an inverted microscope. Morphological characteristics of a single nanoparticle are observed by AFM, and its spectra can be measured from the bottom side. Without any confusion, we can correlate spectral data and morphology, which is impossible by separate scanning electron microscopy (SEM) observation and microspectroscopy as done in the conventional way. By applying this system to perylene nanocrystals, we found an interesting nano-size effect on fluorescence properties. It is well known that conventional perylene crystals larger than μm give only excimer emission, but the monomer emission appears more appreciably and the excimer peak shifts to blue as the size decreases [82]. These deviations from the bulk optical properties were observed for nanocrystals with a size of less than 300 nm.

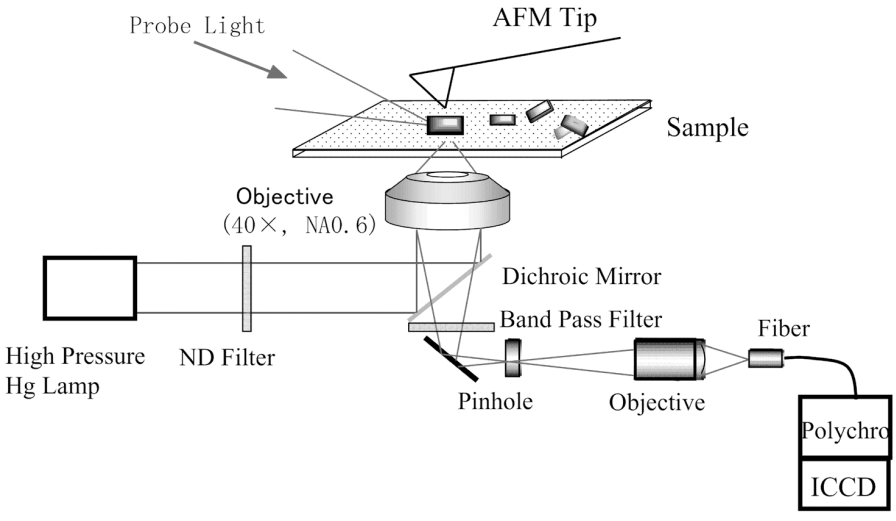

Fig. 5 Experimental set-up for single nanoparticle spectroscopy.

When materials are nonfluorescent, electronic absorption answers the question of electronic excited states, but for individual nanocrystals, the optical path length available for absorption measurements is too short. Moreover, stray light is involved to a great extent, as the probe light cannot be focused to the nm order. Instead of absorption, we proposed to detect the Rayleigh light-scattering spectrum, since it is closely related to the absorption spectrum, as described in textbooks on electromagnetic theory. A fluorescence detection system is used for the scattering measurement, while the value of the scattering coefficient remains in question. It was confirmed for single gold nanoparticles that 30 nm is about the minimum size which gives a reasonable enough signal-to-noise ratio [83]. The result on nanocrystals of polydiacetylene derivatives is shown in Fig. 6 as an example. Each crystal with different shape and size does not give us identical spectra, whose data were arranged as a function of cross-section of rod-like and fibrous crystals [84]. Once again, it was demonstrated that the important dimension is a few tens of nm.

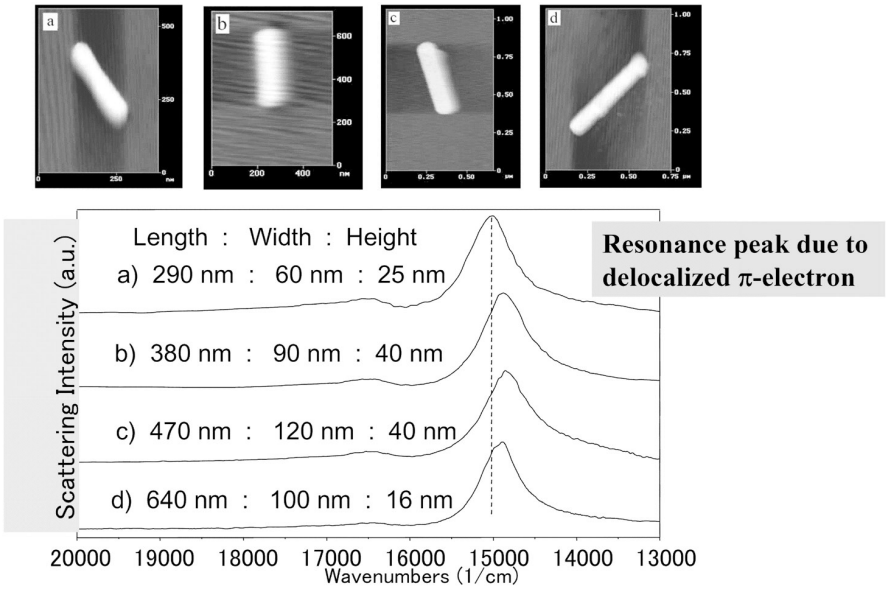

Fig. 6 Shape and scattering spectra of undivided poly-1,6-di(*N*-carbazolyl)hexa-2,4-diyne nanocrystals [84].

It is well known that electron confinement on semiconductor and metal nanodots is observed in the region of a few nm and the Mie-scattering effect is, of course, in the wavelength order. In organic molecules, electrons are confined in small dimensions, so that electronic spectra of molecular systems should not be detected. However, we can conclude on the basis of these results on perylene and diacetylene nanocrystals that a nano-size effect upon optical properties is observed in the larger dimension than that expected. At the present stage of investigation, the new size effect is ascribed to structural confinement. Namely, softening of crystal lattice and packing effect can explain the size dependences of perylene and substituted polydiacetylene, respectively. In addition, conformational distribution of polymer chains is responsible to the nano-size dependence absorption and fluorescence spectra of substituted polythiphenes, which is also a structural confinement [85].

Femtosecond Rayleigh light-scattering spectroscopy of single nanoparticles

If the above Rayleigh scattering detection system is combined with the pump–probe method, its femtosecond measurement is made possible. Indeed, we demonstrated the measurement of electron–phonon and phonon–phonon relaxation dynamics of single gold nanoparticles and found the rate of those relaxations is a few ps and a few hundred ps, respectively [86].

TIME-RESOLVED SPECTROSCOPY AND IMAGING OF NONLINEAR PHOTOCHEMICAL PROCESSES: FROM LASER ABLATION TO PROTEIN CRYSTALLIZATION

Laser ablation is not simple vaporization and sublimation of molecules and atoms from material surface, but fragment ejection characteristic of intense pulsed laser irradiation. It is a nonlinear photochemical behavior which has a threshold value with respect to laser fluence. Thus, laser ablation is induced only by intense laser excitation and never brought about by very long irradiation with continuous wave (CW) laser. Most of the studies were concerned with metals, semiconductors, ceramics, and glasses, while organic materials and bio-related systems were rather limited. The ablation mechanism of organic systems has been considered to be photochemical or photothermal. The higher excited states

formed by intense pulse excitation undergo decomposition to small molecules, and the solid phase is changed to liquid and then to gas phase under an idealized condition.

On the other hand, when the relaxation to the ground electronic state is fast, excitation energy is converted into heat, and high local temperature of the irradiated area may lead to explosive melting, leading to fragmentation and ejection. In general, it is not easy to conclude on the mechanism, as ablation behavior is dependent on laser fluence, wavelength, pulse width, repetition rate, and total shots of laser pulses, and further on materials properties as well as their surface and environmental conditions. Most of the studies had been done for practical applications, so that mechanistic studies were rather rare. We considered that the pump–probe experiment is necessary and indispensable to reveal how electronic excitation energy is used for material ejection, what chemical species are involved, and in what time scale electronic excitation evolves to morphological changes. Such spectroscopic measurements were combined with newly developed time-resolved imaging whose results have given us better pictures of laser ablation dynamics and mechanism at the molecular level.

Molecular mechanism of nanosecond photothermal laser ablation

In order to correlate primary processes of laser ablation with well-known photophysical and photochemical properties, we chose aromatic molecules such as biphenyl, anthracene, or pyrene, and doped them in polymer films or chemically bonded to the polymer [87–114]. Ablation is initiated by absorption of excitation photons by the dopants, and the dynamics were studied by applying time-resolved absorption and fluorescence spectroscopy, transmittance measurement at excitation wavelength, time-of-flight mass spectroscopy, nanosecond shadowing, and photoacoustic measurements. No appreciable decomposition products indicating a photochemical ablation mechanism were detected, and photothermal conversion was considered to be responsible to fragmentation. The surface morphology after ablation suggested melting, the temperature elevation was supported by fluorescence spectral broadening and by kinetic analysis with mass spectrometry, dopant molecules were not decomposed, and excited states were detected spectroscopically. These experimental results indicate that the absorbing molecules convert electronic excitation energy into intermolecular and lattice vibrations very efficiently without chemical decomposition of dopants.

We demonstrated that excited singlet, triplet, and/or ion radicals of the dopants densely formed at the early stage of an excitation pulse of a few tens of ns width absorb the excitation photons at its later stage. The prepared higher excited state relaxes quickly to the first excited states in the time scale of 10 ps, overcoming chemical decomposition. On the other hand, the lowest excited state comes back to the ground state in a few ns. This means that photochemical decomposition is less probable and that the excited state is never bleached while the ground state can be depleted. Examining these processes, we proposed a "cyclic multiphotonic absorption mechanism", schematically shown in Fig. 7, responsible for the efficient nanosecond photothermal conversion [100]. Once we estimated how many photons can be absorbed per dopant in polymer film by time-resolved transmittance measurement at the excitation wavelength, and found 28 for anthracene in polystyrene [101]. It is surprising at first glance, but this is the origin of the rapid temperature elevation and thermal fragmentation. Actually, the fluorescence spectrum of pyrene is initially similar to that observed at a weak excitation condition, but it later becomes very broad, supporting temperature elevation [105].

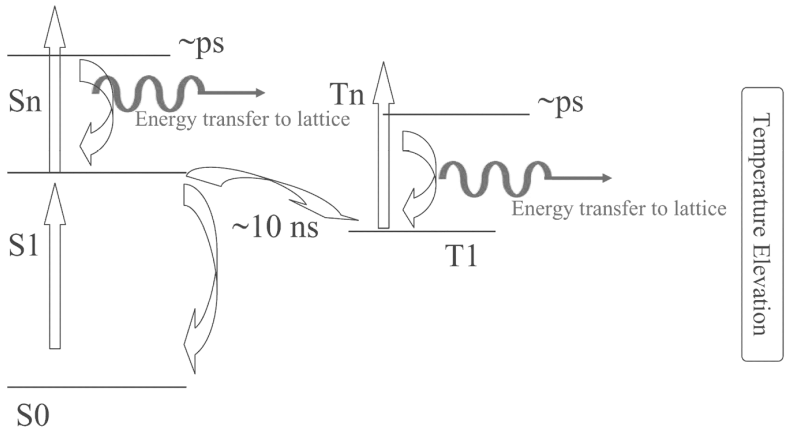

Fig. 7 Cyclic multiphotonic absorption mechanism for nanosecond laser ablation of doped polymer films. As an extreme case, one anthracene in polystyrene film can absorb 28 photons during an excimer laser pulse.

Nanosecond time-resolved interferometric studies

As described above, ablation is a nonlinear behavior with respect to laser fluence, and, in general, below the threshold nothing was left on the surface. However, no trial was done to elucidate the morphological behavior below the threshold before we developed time-resolved interferometry and applied it to interrogate the laser-induced expansion dynamics of polymer films [102,107,108,111–120]. Our system is given in Fig. 8, where a nanosecond probe pulse is used to generate interferograms at different delay times after the nanosecond excitation. The periodic pattern of the interferogram shifts when polymer films undergo expansion, contraction, and ablation, from which the surface displacement can be numerically estimated. The time and space (in this case, vertical displacement of the surface) resolutions of our system are 10 ns and 13 nm, respectively. Results on a poly(methyl methacrylate) film are shown in Fig. 9 as an example, where the expansion proceeded as an integral of the excitation pulse, meaning that the expansion of the film takes place on the order of 10 ns. Later, the film underwent contraction and gave permanent swelling. We could assure the heating and cooling dynamics by observing these nanometer expansion and contraction behaviors. One more interesting result is that the behavior represents the time scale of glass-rubber phase transition. In the case of this film, the expansion coefficient above a certain laser fluence is larger than that below it, and the fluence giving this knick point corresponds to the temperature of the transition [107,116]. When the expansion above the fluence was observed, we found that the rise curve was delayed compared to the integrated one of the excitation pulse, and its delay being of about 10 ns. This suggests that the phase transition occurs in the time scale of 10 ns, which is the first experimental data of the direct observation of the phase transition. The ns and nm dynamic analysis by interferometry is very useful to obtain dynamic aspects of such morphological changes.

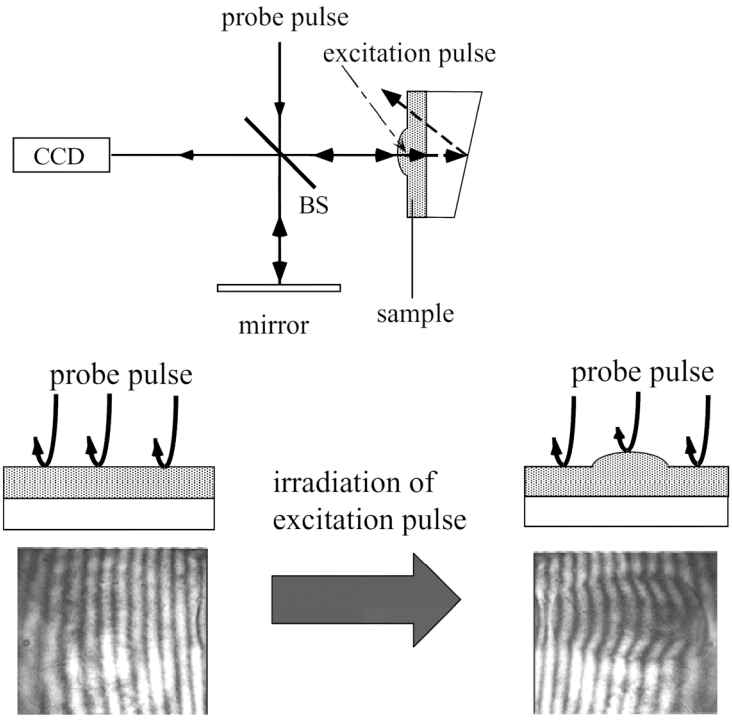

Fig. 8 Nanosecond time-resolved interferometric measurement where the amplitude of surface displacement can be estimated from fringe shifts and arranged as a function of delay time. Excitation pulse is from the excimer laser or OPO system, while a probe pulse is 2nd harmonics of Nd^{3+}:YAG laser (532 nm, 10 ns fwhm).

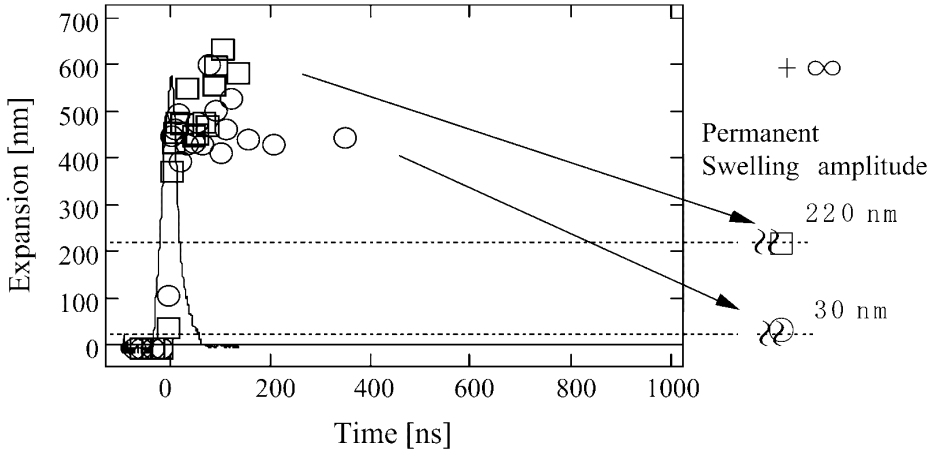

Fig. 9 Expansion and contraction dynamics of PMMA films at the fluence of 1100 mJ cm^{-2} (□) and 870 mJ cm^{-2} (○) between the swelling and ablation thresholds. Arrows indicate the time range where the fringe pattern of interference images of the irradiated area cannot be observed by the darkening fragmented debris. A solid curve represents a typical excimer laser pulse.

Photochemical laser ablation of polymer films

Although photothermal processes are important in polymer films as described above, some polymers having photodecomposable groups in the main chain undergo ablation instantaneously [121–128]. It was confirmed by nanosecond interferometry that etching starts during the excitation pulse of a few tens of ns.

Photochemical laser ablation of liquid benzene derivatives

As photochemists, we wished to find molecular systems where pure photochemical reactions evolve into fragmentation and ejection of materials. We started from the nanosecond studies on liquid benzene derivatives, as their photochemical properties are well known [129–134]. Then we developed a femtosecond laser system giving a high-intensity pulse at 254 nm and applied it to the same liquid benzene derivatives [135–139]. In addition to femtosecond absorption spectroscopy, we more recently developed a femtosecond surface light-scattering imaging method, which monitors the morphological primary processes occurring at the liquid surface before ejection. If the surface becomes rough and scatters the light by intense laser excitation, the monitoring light can in turn be detected at any angle, giving the roughened area as a bright one. The image observed as a function of delay time gives dynamic evolution of surface morphological changes. Upon intense femtosecond excitation, the benzyl radical was spectroscopically confirmed and then surface roughening was detected. This indicates that photodecomposition induces ablation, and its threshold was related to photochemical reactivity of benzyl radical formation of this series of molecules. This is also an example showing the direct evolution from photochemical decomposition to material ejection. However, laser ablation is very complex, and we found that in the case of toluene, the radical was not observed and photothermal ablation involving the triplet state was spectroscopically demonstrated.

Femtosecond photomechanical laser ablation mechanism

It had been widely believed that intense ultrashort light pulse excitation results in plasma formation, causing ablation phenomena. This may be applied to metals and semiconductors, but we doubted that this plasma is responsible for the ablation of molecular materials. We applied femtosecond absorption spectroscopy and femtosecond surface light-scattering imaging to phthalocyanine films and subsequently revealed the primary electronic and morphological processes [140–143]. We could not detect ionic species of phthalocyanine molecules as main components, therefore, we may be able to exclude the possibility of a plasma mechanism, since some kinds of ionic phthalocyanine should be observed at least at the initial stage of ablation in case of plasma formation. It was clear that the primary component was the exciton of phthalocyanine, soon replaced in 20 ps by a hot band of the ground electronic state. This was interpreted by mutual interactions between excitons inducing the sudden temperature elevation, and its degree was estimated by comparing transient absorption spectra with the temperature difference spectra. It is worth noting that quite normal dynamics of the excited states are detected. Finally, the problem is how to correlate these electronic processes to fragmentation.

The surface roughness just before fragmentation starts was probed by time-resolved surface light-scattering imaging. The root-mean-squared roughness of phthalocyanine films increased up to a few tens of nm only after 10 ns, although the film was excited by 170 fs laser pulses. The temperature elevation was attained after 20 ps following excitation as mentioned before, while the surface morphology change was not clearly detected before 10 ns. This suggests that vigorous intramolecular and lattice vibrations are enhanced and confined in the irradiated area for 20 ps to 10 ns delay time, which may be represented as a transient pressure. The irradiated part is surrounded by unexcited film and substrate glass, and thermal conduction is not fast, so that the pressure is released by fragmentation of the film to open air. The whole irradiated part has large energy, and the whole momentum should be compensated

in the area, only an upper part is ejected and the lower part is left. This explanation is in agreement with the experimental etching result, which is quite different from nanosecond laser ablation. Therefore, we have proposed that a photomechanical mechanism operates for femtosecond laser ablation of molecular materials.

Nanoparticle formation by solution ablation

Laser ablation studies have been more or less conducted for developing microfabrication methodology, and it was revealed in detail how precisely and finely the surface morphology was prepared. However, it is also necessary to pay attention to ejected materials. First, we observed the ejected particles by landing them softly on polymer films, which were overlaid on irradiated molecular materials [144]. Small particles with size of less than a μm are usually observed on the polymer film, which gave us the following idea: If the ablation is performed in an inert solvent, ejected particles might be dispersed in the solvent. Fortunately, we were able to prepare nanocolloids just by inducing laser ablation of dispersed molecular microcrystals. We have succeeded so far in fabricating nanoparticles of various dyes [145–149], and can say at present that laser ablation in inert solvents is one of most useful methods for nanoparticle preparation.

The representative example shown in Fig. 10 is the result on quinacridone (QA), where it is seen that the size before and after irradiation was a few μm and a few tens of nm, respectively. The minimum size of this dye nanoparticle is 13 nm when the 800 nm femtosecond laser was applied. The laser parameters such as wavelength, pulse width, laser fluence, repetition rate, and shot number can be tuned to prepare many nanoparticles of various sizes, shapes, and phases in the case of crystals. Furthermore, temperature and solvent with different thermal conductivity are useful factors to optimize the preparation process.

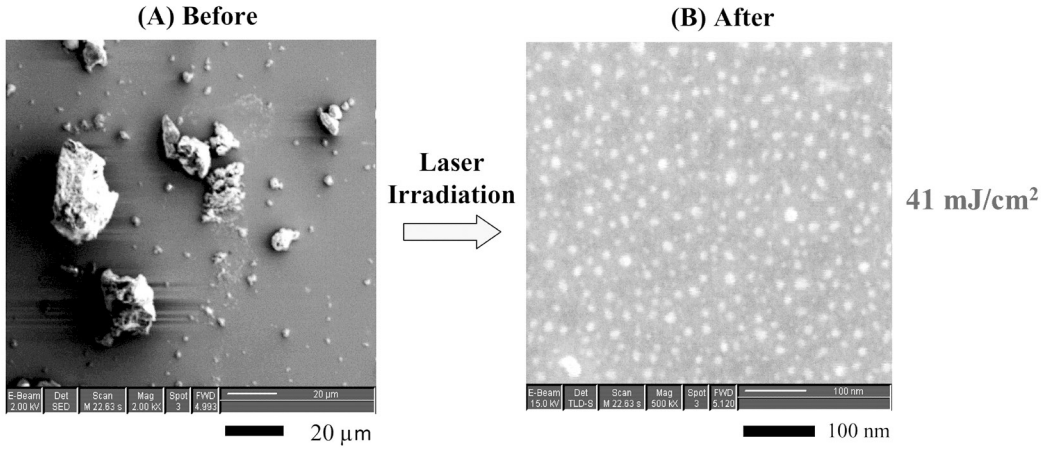

Fig. 10 (A) SEM image of initial QA microcrystals after sonication. (B) SEM images of QA nanoparticles after laser irradiation. Conditions: laser fluence, 41 mJ/cm^2; irradiation time, 150 min.

Crystal growth control with femtosecond laser ablation

The ejected small fragment and/or etched surface will be a crystal nucleus from which crystal can be grown in saturated solution. This unconventional idea was demonstrated by irradiating a urea crystal in water with a single femtosecond pulse [150]. A certain spot of the crystal should be ablated, and we observed surprisingly a crystal growing from that spot. The single fiber-like crystal grew almost perpendicular to the mother crystal at a rate of 100 μm s^{-1}, and during growth, some convection of the solu-

tion was detected. If the femtosecond intensity was increased, plural fibers were obtained. Thus, sequential irradiation of the formed crystals creates some three-dimensional crystal structures, as demonstrated in Fig. 11. It is worth noting that the crystal growth is observed only for femtosecond irradiation, and, if a CW near-infrared laser is applied, the irradiated area melts, followed by re-crystallization after switching off the laser.

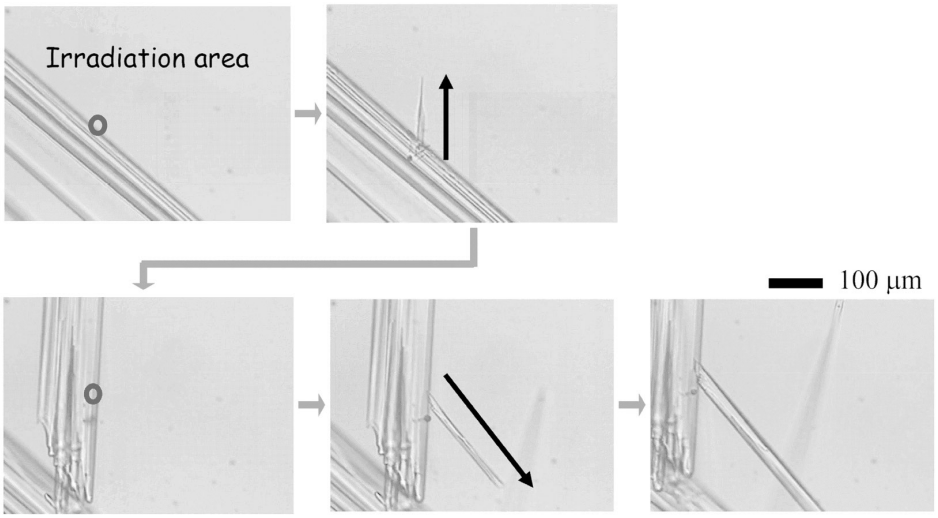

Fig. 11 Spatial control of urea crystal growth in its saturated solution by one-shot femtosecond laser irradiation (1.2 mJ/pulse, 800 nm) ×10 N.A. 0.4.

Femtosecond laser-induced crystallization

As we found quite recently, sometimes crystals are prepared only by irradiating a saturated solution of molecules with a femtosecond laser pulse. This unique phenomenon is closely related with nonlinear photophysical and photochemical processes induced by femtosecond laser excitation; shockwave generation and propagation; plasma formation; and cavitation bubbling. In water, their thresholds were estimated by observing these phenomena with different laser fluence. The lowest fluence increases in the order of shockwave < plasma formation < cavitation, and, taking advantage of these phenomena, we have developed very interesting tools and methodologies for molecular and biological sciences. For single living cells, we have proposed a new manipulation method [151,152], demonstrating how to remove them from the culture media, how to pattern them on a substrate, and how to inject unconventional nanoparticles into them. Presently, as a photochemical application we describe crystallization dynamics.

It is widely known that it is not easy to crystallize proteins as they have large molecular weights and wide conformational distributions. Many trials have been systematically extended, while our approach is to induce cavitation bubbling by focusing a femtosecond laser pulse to a supersaturated solution of protein [153–156]. It was evidenced that larger single crystals with better qualities were prepared, compared to those grown in the absence of irradiation. Even when the simple lysozyme was examined, crystallization occurred in a few days, so that a dynamic and mechanistic study on laser-induced crystallization is difficult to achieve. Consequently, we chose urea and anthracene as model samples as they crystallize rapidly, and observed crystallization behavior by time-resolved imaging. This pump–probe experiment reveals that the contribution of the femtosecond laser-induced bubbling is a key for crystallization, whose study is in progress in our group.

SUMMARY AND PERSPECTIVE

Time-resolved reflection and single nanoparticle spectroscopies have been developed and applied to the elucidation of photophysical and photochemical processes of nanomaterials. Now these studies can be concluded at the level of studies on gas and solution phases. Typical processes such as intersystem crossing, electron transfer and recombination, isomerization, and so on were revealed for films and powders, while exciton–exciton annihilation leading to temperature elevation was confirmed to be a characteristic process of surface/interface layers of molecular films. This is closely related to laser ablation when the laser fluence is higher than a certain threshold. Nanosecond and femtosecond laser ablation mechanisms are proposed, for which interesting systematic studies from nanoparticle properties to protein crystallization were started.

In addition to the present topics described here, new chemistry research on mechanical force effect on polymers, colloids, cells, and other systems in solution is opened by the combination of lasers and microscopes. A focused near-infrared laser beam exerts a photon force on micro/nanomaterials, enabling their manipulation. The optical trapping studies have been conducted by physicists, while the extension to chemistry was started by us. The minimum size of the trapped particles in solution at room temperature was confirmed to be a few nm. The force is strong enough to suppress electrostatic repulsion between electrolytes and to break the hydrogen-bonding network around polymers in water. Larger photon forces are exerted on molecules with higher polarizability. Such molecular structure-photon force relation opened a new field that could be coined "chemistry of photon force" [5–7].

This is further being extended to trapping dynamics of single micro/nanoparticles in solution at room temperature [7,157]. For 100-nm-sized particles, successive trapping could be followed for smaller particles, while photon-force assisted-aggregation was clearly confirmed. Furthermore, absolute potential shape of an optical trapping-well was determined by directly measuring fluctuations of a single probing microparticle in solution, while spectroscopic identification of assembled structures in the trapping potential was done for model gold nanoparticles. By the 3-dimensional trapping and manipulation of nanoparticles and their fixation onto substrate, the nanoparticles were aligned with a resolution of a few tens of nm. Although the spatial resolution is less than that of the 2-dimensional surface manipulation by a scanning tunneling microscope (STM) tip at low temperature under vacuum, the much broader applicability is very important for biological material, cells, and protein crystals.

Photochemistry in the nanodimension is made successful by developing various time-resolved spectroscopy, imaging, microscopy, and interferometry; by analyzing the dynamics and mechanisms of conventional primary processes, laser-induced morphological changes, and crystallization in small domains; and by integrating the photon force effect. It is indeed productive and is opening up various new research fields.

ACKNOWLEDGMENTS

The authors are very much indebted to the collaborators listed in the references. In particular, Prof. Hiroshi Fukumura, who was a member of our laboratory and now is a professor at Tohoku University, is greatly acknowledged for his excellent contribution. The present work is partly supported by a Grant-in-Aid for Scientific Research (KAKENHI) on the priority area "Molecular Nano Dynamics" (16072211) from the Ministry of Education, Culture, Sports, Science, and Technology of Japan (MEXT).

REFERENCES

1. H. Masuhara. *Pure Appl. Chem.* **64**, 1279 (1992).
2. H. Masuhara. *J. Photochem. Photobiol., A* **62**, 397 (1992).
3. H. Masuhara, N. Kitamura, H. Misawa, K. Sasaki, M. Koshioka. *J. Photochem. Photobiol., A* **65**, 235 (1992).
4. H. Masuhara, F. C. De Schryver, N. Kitamura, N. Tamai (Eds.). *Microchemistry: Spectroscopy and Chemistry in Small Domains*, North Holland/Elsevier, Amsterdam (1994).
5. H. Masuhara, F. C. De Schryver (Eds.). *Organic Mesoscopic Chemistry* (IUPAC 21st Century Chemistry Monograph), Blackwell Science, Oxford (1999).
6. H. Masuhara, H. Nakanishi, K. Sasaki (Eds.). *Single Organic Nanoparticles*, Springer, Berlin (2003).
7. H. Masuhara, S. Kawata (Eds.). *Nanophotonics: Integrating Photochemistry, Optics and Nano/Bio Materials Studies*, Elsevier, Amsterdam (2004).
8. G. Porter. *Chemistry in Microtime*, Imperial College Press, London (1997).
9. A. H. Zewail. *Femtochemistry: Ultrafast Dynamics of the Chemical Bond*, Vols. 1 and 2, World Scientific, Singapore (1994).
10. R. Srinivasan, W. J. Leigh. *J. Am. Chem. Soc*. **104**, 6784 (1982).
11. H. Masuhara, N. Mataga, S. Tazuke, T. Murao, I. Yamazaki. *Chem. Phys. Lett.* **100**, 415 (1983).
12. Y. Taniguchi, M. Mitsuya, N. Tamai, I. Yamazaki, H. Masuhara. *J. Colloid Interface Sci.* **104**, 596 (1985).
13. H. Masuhara, S. Tazuke, N. Tamai, I. Yamazaki. *J. Phys. Chem*. **90**, 5830 (1986).
14. A. Kurahashi, A. Itaya, H. Masuhara, M. Sato, T. Yamada, C. Koto. *Chem. Lett.* **15**, 1413 (1986).
15. A. Itaya, A. Kurahashi, H. Masuhara, N. Tamai, I. Yamazaki. *Chem. Lett.* **16**, 1079 (1987).
16. M. Toriumi, M. Yanagimachi, H. Masuhara. *Proc. SPIE-Int. Soc. Opt. Eng.* **1466**, 458 (1991).
17. M. Toriumi, H. Masuhara. *Spectrochim. Acta Rev*. **14**, 353 (1991).
18. M. Yanagimachi, M. Toriumi, H. Masuhara. *Chem. Mater.* **3**, 413 (1991).
19. M. Yanagimachi, M. Toriumi, H. Masuhara. *Appl. Spectrosc.* **46**, 832 (1992).
20. M. Toriumi, M. Yanagimachi, H. Masuhara. *Appl. Opt.* **31**, 6376 (1992).
21. M. Yanagimachi, N. Tamai, H. Masuhara. *Chem. Phys. Lett*. **200**, 469 (1992).
22. M. Yanagimachi, N. Tamai, H. Masuhara. *Chem. Phys. Lett*. **201**, 115 (1993).
23. S. Hamai, N. Tamai, H. Masuhara. *Chem. Lett*. **7**, 1105 (1993).
24. S. Hamai, N. Tamai, H. Masuhara. *Chem. Phys. Lett*. **213**, 407 (1993).
25. S. Hamai, N. Tamai, H. Masuhara. *Chem. Phys. Lett*. **229**, 389 (1994).
26. S. Hamai, N. Tamai, H. Masuhara. *J. Phys. Chem*. **99**, 4980 (1995).
27. N. Ikeda, T. Kuroda, H. Masuhara. *Chem. Phys. Lett.* **156**, 204 (1989).
28. R. W. Kessler, F. Wilkinson. *J. Chem. Soc., Faraday Trans. 1* **77**, 309 (1981).
29. K. Imagi, N. Ikeda, H. Masuhara, M. Nisigaki, M. Isogawa. *Polymer J.* **19**, 999 (1987).
30. N. Ikeda, K. Imagi, H. Masuhara, N. Nakashima, K. Yoshihara. *Chem. Phys. Lett.* **140**, 281 (1987).
31. N. Ikeda, M. Koshioka, H. Masuhara, K. Yoshihara. *Chem. Phys. Lett.* **150**, 452 (1988).
32. N. Ikeda, M. Koshioka, H. Masuhara, N. Nakashima, Y. Yoshihara. *Ultrafast Phenomena VI*, pp. 428–430, Springer-Verlag, New York (1989).
33. N. Ikeda, T. Hara, H. Masuhara. *Chem. Lett.* 683 (1990).
34. M. Koshioka, H. Mizuma, K. Imagi, N. Ikeda, H. Fukumura, H. Masuhara. *Bull. Chem. Soc. Jpn.* **63**, 3495 (1990).
35. M. Koshioka, N. Ikeda, A. Itaya, H. Masuhara. *Chem. Lett.* 1165 (1992).
36. H. Mizuma, H. Fukumura, H. Masuhara. *Photochem. Photobiol*. **58**, 777 (1993).
37. N. Fukazawa, K. Yoshioka, H. Fukumura, H. Masuhara. *J. Phys. Chem.* **97**, 6753 (1993).

38. S. Yamamoto, H. Mizuma, A. Nitta, N. Fukazawa, H. Fukumura, H. Masuhara. *Chem. Phys. Lett.* **215**, 323 (1993).
39. S. Hashimoto, N. Fukazawa, H. Fukumura, H. Masuhara. *Chem. Phys. Lett*. **219**, 445 (1994).
40. N. Fukazawa, H. Fukumura, H. Masuhara. *Chem. Phys. Lett.* **222**, 123 (1994).
41. S. Hashimoto, N. Fukazawa, H. Fukumura, H. Masuhara. *Chem. Phys. Lett.* **223**, 493 (1994).
42. N. Fukazawa, H. Fukumura, H. Masuhara, J. Prochorow. *Chem. Phys. Lett*. **220**, 461 (1994).
43. S. Hashimoto, T. Mutoh, H. Fukumura, H. Masuhara. *J. Chem. Soc., Faraday Trans.* **92**, 3653 (1996).
44. T. Asahi, Y. Matsuo, H. Masuhara. *Chem. Phys. Lett.* **256**, 525 (1996).
45. H. Koshima, Y. Wang, T. Matsuura, I. Miyahara, H. Mizutani, K. Hirotsu, T. Asahi, H. Masuhara. *J. Chem. Soc., Perkin Trans. 2* 2033 (1997).
46. T. Asahi, Y. Matsuo, H. Masuhara, H. Koshima. *J. Phys. Chem. A* **101**, 612 (1997).
47. S. Takatani, H. Fukumura, H. Masuhara, S. Hashimoto. *J. Phys. Chem. B* **101**, 3365 (1997).
48. T. Asahi, A. Furube, H. Masuhara. *Chem. Phys. Lett.* **275**, 234 (1997).
49. A. Furube, T. Asahi, H. Masuhara, H. Yamashita, M. Anpo. *Chem. Lett.* **27**, 735 (1997).
50. T. Asahi, H. Masuhara. *Chem. Lett.* **26**, 1165 (1997).
51. T. Asahi, A. Furube, H. Fukumura, M. Ichikawa, H. Masuhara. *Rev. Sci. Instrum.* **69**, 361 (1998).
52. T. Asahi, K. Kibisako, H. Masuhara, H. Kasai, H. Katagi, H. Oikawa, H. Nakanishi. *Mol. Cryst. Liq. Cryst.* **314**, 95 (1998).
53. T. Asahi, A. Furube, H. Masuhara. *Bull. Chem. Soc. Jpn.* **71**, 1277 (1998).
54. A. Furube, T. Asahi, H. Masuhara, H. Yamashita, M. Anpo. *J. Phys. Chem. B* **103**, 3120 (1999).
55. S. Hashimoto, N. Hagiwara, T. Asahi, H. Masuhara. *Langmuir* **15**, 3123 (1999).
56. A. Furube, T. Asahi, H. Masuhara. *Jpn. J. Appl. Phys*. **38**, Part 1, 4236 (1999).
57. M. Suzuki, T. Asahi, H. Masuhara. *Mol. Cryst. Liq. Cryst.* **345**, 51 (2000).
58. A. Furube, T. Asahi, H. Masuhara, H. Yamashita, M. Anpo. *Res. Chem. Intermed.* **27**, 177 (2001).
59. A. Furube, T. Asahi, H. Masuhara, H. Yamashita, M. Anpo. *Chem. Phys. Lett.* **336**, 424 (2001).
60. H. Nishiguchi, J.-L. Zhang, M. Anpo, H. Masuhara. *J. Phys. Chem. B* **105**, 3218 (2001).
61. Y. Kim, J. R. Choi, M. Yoon, A. Furube, T. Asahi, H. Masuhara. *J. Phys. Chem. B* **105**, 8513 (2001).
62. M. Suzuki, T. Asahi, H. Masuhara. *Phys. Chem. Chem. Phys*. **4**, 185 (2002).
63. S. Link, A. Furube, M. B. Mohamed, T. Asahi, H. Masuhara, M. A. El-Sayed. *J. Phys. Chem. B* **106**, 945 (2002).
64. T. Asahi, M. Suzuki, H. Masuhara. *J. Phys. Chem. A* **106**, 2335 (2002).
65. M. Suzuki, T. Asahi, K. Takahashi, H. Masuhara. *Chem. Phys. Lett*. **368**, 384 (2002).
66. S. Y. Ryu, M. Yoon, J. H. Choy, S. H. Hwang, A. Frube, T. Asahi, H. Masuhara. *Bull. Korean Chem. Soc.* **24**, 446 (2003).
67. T. Asahi, H. Masuhara, K. Nakatani, M. Sliwa. *Mol. Cryst. Liq. Cryst.* **431**, 541 (2005).
68. M. Suzuki, T. Asahi, H. Masuhara. *ChemPhysChem* **6**, 2396 (2005).
69. M. Ichikawa, H. Fukumura, H. Masuhara. *J. Phys. Chem*. **98**, 12211 (1994).
70. M. Ichikawa, H. Fukumura, H. Masuhara, A. Koide, H. Hyakutake. *Chem. Phys. Lett*. **232**, 346 (1995).
71. M. Ichikawa, H. Fukumura, H. Masuhara. *J. Phys. Chem*. **99**, 12072 (1995).
72. H. Fukumura, Y. Yoneda, H. Takahashi, H. Masuhara. *Chem. Lett.* **25**, 509 (1996).
73. Y. Hosokawa, K. Watanabe, T. Asahi, H. Fukumura, H. Masuhara, Y. Imanishi. *Mol. Cryst. Liq. Cryst.* **314**, 64 (1998).
74. Y. Hosokawa, K. Watanabe, T. Asahi, H. Fukumura, H. Masuhara. *Bull. Chem. Soc. Jpn.* **72**, 909 (1999).
75. H. Van Mingroot, L. Viaene, M. Van der Auweraer, F. C. De Schryver, M. Ichikawa, H. Fukumura, H. Masuhara. *J. Phys. Chem*. **99**, 17174 (1995).
76. N. Tamai, T. Asahi, H. Masuhara. *Chem. Phys. Lett.* **198**, 413 (1992).

77. T. Asahi, N. Tamai, T. Uchida, N. Shimo, H. Masuhara. *Chem. Phys. Lett*. **234**, 337 (1995).
78. K. Sasaki, M. Koshioka, H. Masuhara. *Appl. Spectrosc*. **45**, 1041 (1991).
79. K. Kamada, K. Sasaki, H. Misawa, N. Kitamura, H. Masuhara. *Chem. Phys. Lett.* **210**, 89 (1993).
80. N. Tamai, T. Asahi, H. Masuhara. *Rev. Sci. Instrum*. **64**, 2496 (1993).
81. C. F. Porter, N. Tamai, H. Masuhara. *Laser Chem.* **16**, 197 (1996).
82. H. Matsune, T. Asahi, H. Masuhara, H. Kasai, H. Nakanishi. *MRS Symp. Proc.* **846**, DD10.8.1-6 (2005).
83. T. Itoh, T. Asahi, H. Masuhara. *Jpn. J. Appl. Ph*ys. **41**, Part 2, L76 (2002).
84. V. Volkov, T. Asahi, H. Masuhara, A. Masuhara, H. Kasai, H. Oikawa, H. Nakanishi. *J. Phys. Chem. B* **108**, 7674 (2004).
85. N. Kurokawa, H. Yoshikawa, N. Hirota, K. Hyodo, H. Masuhara. *ChemPhysChem* **5**, 1609 (2004).
86. T. Itoh, T. Asahi, H. Masuhara. *Appl. Phys. Lett.* **79**, 1667 (2001).
87. H. Masuhara, H. Hiraoka, K. Domen. *IBM Res. J.* 55174 (1986).
88. H. Masuhara, H. Hiraoka, K. Domen. *Macromolecules* **20**, 450 (1987).
89. H. Masuhara, H. Hiraoka, E. E. Marinero. *Chem. Phys. Lett.* **135**, 103 (1987).
90. H. Hiraoka, T. J. Chuang, H. Masuhara. *J. Vac. Soc. Technol., B* **6**, 463 (1988).
91. H. Masuhara, S. Eura, H. Fukumura, A. Itaya. *Chem. Phys. Lett.* **156**, 446 (1989).
92. A. Itaya, A. Kurahashi, H. Masuhara, Y. Taniguchi, M. Kiguchi. *J. Appl. Phys.* **67**, 2240 (1990).
93. H. Masuhara, H. Fukumura. *Polymer News* **17**, 5 (1991).
94. H. Fukumura, N. Mibuka, S. Eura, H. Masuhara. *Appl. Phys. A* **53**, 255 (1991).
95. H. Fukumura, K. Hamano, S. Eura, H. Masuhara, H. Ito, T. Sakakibara, M. Matsuda. *Chem. Phys. Lett.* **194**, 203 (1992).
96. H. Fukumura, H. Masuhara. *J. Photopolym. Sci. Technol*. **5**, 223 (1992).
97. H. Fukumura, K. Hamano, H. Masuhara. *Chem. Lett.* 245 (1993).
98. H. Fukumura, K. Hamano, H. Masuhara. *J. Phys. Chem*. **97**, 12110 (1993).
99. H. Fukumura, N. Mibuka, S. Eura, H. Masuhara, N. Nishi. *J. Phys. Chem*. **97**, 13761 (1993).
100. H. Fukumura, H. Masuhara. *Chem. Phys. Lett.* **221**, 373 (1994).
101. H. Fujiwara, T. Hayashi, H. Fukumura, H. Masuhara. *Appl. Phys. Lett*. **64**, 2451 (1994).
102. H. Furutani, H. Fukumura, H. Masuhara. *Appl. Phys. Lett*. **65**, 3413 (1994).
103. H. Fukumura, E.-I. Takahashi, H. Masuhara. *J. Phys. Chem*. **99**, 750 (1995).
104. H. Fujiwara, Y. Nakajima, H. Fukumura, H. Masuhara. *J. Phys. Chem*. **99**, 11481 (1995).
105. H. Fujiwara, H. Fukumura, H. Masuhara. *J. Phys. Chem.* **99**, 11844 (1995).
106. Y. Tsuboi, S.-I. Sakashita, K. Hatanaka, H. Fukumura, H. Masuhara. *Laser Chem.* **16**, 167 (1996).
107. H. Furutani, H. Fukumura, H. Masuhara. *J. Phys. Chem*. **100**, 6871 (1996).
108. H. Furutani, H. Fukumura, H. Masuhara. *Rev. Laser Eng. (Japanese)* **25**, 288 (1997).
109. M. Hosoda, H. Furutani, H. Fukumura, H. Masuhara, M. Nishii, N. Ichinose, S. Kawanishi. *Rev. Laser Eng. (Japanese)* **25**, 306 (1997).
110. H. Fujiwara, H. Fukumoto, H. Fukumura, H. Masuhara. *Res. Chem. Intermed.* **24**, 879 (1998).
111. T. Tada, T. Asahi, H. Masuhara, M. Tsuchimori, O. Watanabe. *J. Photosci*. **10**, 97 (2003).
112. H. Fujiwara, H. Ishii, T. Ishiwata, T. Hayashi, H. Fukumura, H. Masuhara. *Bull. Chem. Soc. Jpn*. **76**, 1075 (2003).
113. T. Tada, T. Asahi, M. Tsuchimori, O. Watanabe, H. Masuhara. *Jpn. J. Appl. Phys.* **45**, 5337 (2004).
114. T. Tada, T. Asahi, M. Tsuchimori, O. Watanabe, H. Masuhara. *J. Nonlinear Opt. Phys. Mater.* **13**, 373 (2004).
115. T. Masubuchi, H. Furutani, H. Fukumura, H. Masuhara. *ChemPhysChem* **3**, 137 (2000).
116. T. Masubuchi, H. Furutani, H. Fukumura, H. Masuhara. *J. Phys. Chem. B* **105**, 2518 (2001).
117. T. Masubuchi, H. Fukumura, H. Masuhara, K. Suzuki, N. Hayashi. *J. Photochem. Photobiol., A* **145**, 215 (2001).

118. T. Masubuchi, T. Tada, E. Nomura, K. Hatanaka, H. Fukumura, H. Masuhara. *J. Phys. Chem. A* **106**, 2180 (2002).
119. T. Mito, T. Masubuchi, T. Tada, H. Fukumura, H. Masuhara. *J. Photosci.* **6**, 109 (1999).
120. T. Mito, H. Masuhara. *Appl. Surf. Sci.* **197–198**, 796 (2002).
121. L. S. Bennett, T. Lippert, H. Furutani, H. Fukumura, H. Masuhara. *Appl. Phys. A* **63**, 327 (1996).
122. T. Lippert, L. S. Bennett, T. Kunz, C. Hahn, A. Wokaun, H. Furutani, H. Fukumura, H. Masuhara, T. Nakamura, A. Yabe. *Proc. SPIE-Int. Soc. Opt. Eng.* **2992**, 135 (1997).
123. H. Fukumura, H. Masuhara, T. Lippert, A. Yabe. *J. Phys. Chem. A* **101**, 5742 (1997).
124. H. Furutani, H. Fukumura, H. Masuhara, S. Kambara, T. Kitaguchi, H. Tsukada, T. Ozawa. *J. Phys. Chem. B* **102**, 3395 (1998).
125. T. Lippert, J. T. Dickinson, S. C. Langford, H. Furutani, H. Fukumura, H. Masuhara, T. Kunz, A. Wokaun. *Appl. Surf. Sci.* **127–129**, 117 (1998).
126. T. Mito, T. Tsujita, H. Masuhara, N. Hayashi, K. Suzuki. *Jpn. J. Appl. Phys*. **40**, Part 2, L805 (2001).
127. T. Lippert, C. David, M. Hauer, T. Masubuchi, H. Masuhara, K. Nomura, O. Nuyken, C. Phipps, J. Robert, T. Tada, K. Tomita, A. Wokaun. *Appl. Surf. Sci.* **186**, 14 (2002).
128. T. Lippert, J. T. Dickinson, M. Hauer, G. Kopitkovas, S. C. Langford, H. Masuhara, O. Nuyken, J. Robert, H. Salmio, T. Tada, K. Tomita, A. Wokaun. *Appl. Surf. Sci.* **197–198**, 746 (2002).
129. Y. Tsuboi, H. Fukumura, H. Masuhara. *Appl. Phys. Lett*. **64**, 2745 (1994).
130. Y. Tsuboi, K. Hatanaka, H. Fukumura, H. Masuhara. *J. Phys. Chem.* **98**, 11237 (1994).
131. Y. Tsuboi, H. Masuhara. *Rev. Laser Eng. (Japanese)* **23**, 9 (1995).
132. Y. Tsuboi, H. Masuhara. *Rev. Laser Eng. (Japanese)* **23**, 2 (1995).
133. Y. Tsuboi, H. Fukumura, H. Masuhara. *J. Phys. Chem.* **99**, 10305 (1995).
134. Y. Tsuboi, K. Hatanaka, H. Fukumura, H. Masuhara. *J. Phys. Chem. A* **102**, 1661 (1998).
135. K. Hatanaka, M. Kawao, H. Fukumura, H. Masuhara. *J. Appl. Phys*. **82**, 5799 (1997).
136. K. Hatanaka, T. Itoh, T. Asahi, N. Ichinose, S. Kawanishi, T. Sasuga, H. Fukumura, H. Masuhara. *Appl. Phys. Lett.* **73**, 3498 (1998).
137. K. Hatanaka, T. Itoh, T. Asahi, N. Ichinose, S. Kawanishi, T. Sasuga, H. Fukumura, H. Masuhara. *Chem. Phys. Lett.* **300**, 727 (1999).
138. K. Hatanaka, T. Itoh, T. Asahi, N. Ichinose, S. Kawanishi, T. Sasuga, H. Fukumura, H. Masuhara. *J. Phys. Chem. A* **103**, 11257 (1999).
139. K. Hatanaka, Y. Tsuboi, H. Fukumura, H. Masuhara. *J. Phys. Chem. B* **106**, 3049 (2002).
140. Y. Hosokawa, M. Yashiro, T. Asahi, H. Masuhara. *Proc. SPIE-Int. Soc. Opt. Eng.* **4274**, 78 (2001).
141. Y. Hosokawa, Masaki Yashiro, T. Asahi, H. Masuhara. *J. Photochem. Photobiol., A.* **142**, 197 (2001).
142. Y. Hosokawa, M. Yashiro, T. Asahi, H. Masuhara, T. Kadota, Y. Shirota. *Jpn. J. Appl. Phys*. **40**, Part 2, L1116 (2001).
143. Y. Hosokawa, T. Asahi, H. Masuhara. *Rev. Laser Eng. (Japanese)* **29**, 710 (2001).
144. T. Asahi, H. Y. Yoshikawa, M. Yashiro, H. Masuhara. *Appl. Surf. Sci.* **197–198**, 777 (2002).
145. Y. Tamaki, T. Asahi, H. Masuhara. *Appl. Surf. Sci.* **168**, 85 (2000).
146. Y. Tamaki, T. Asahi, H. Masuhara. *J. Phys. Chem. A* **106**, 2135 (2002).
147. Y. Tamaki, T. Asahi, H. Masuhara. *Jpn. J. Appl. Phys.* **42**, Part 1, 2725 (2003).
148. T. Sugiyama, T. Asahi, H. Masuhara. *Chem. Lett*. **33**, 724 (2004).
149. T. Sugiyama, T. Asahi, H. Takeuchi, H. Masuhara. *Jpn. J. Appl. Phys.* **45**, Part 1, 384 (2006).
150. H. Y. Yoshikawa, Y. Hosokawa, H. Masuhara. *Cryst. Growth Des.* **6**, 302 (2006).
151. Y. Hosokawa, J. Takabayashi, C. Shukunami, Y. Hiraki, H. Masuhara. *Appl. Phys. A* **79**, 795 (2004).
152. Y. Hosokawa, J.-I. Takabayashi, C. Shukunami, Y. Hiraki, H. Masuhara. *Rev. Laser Eng. (Japanese)* **32**, 94 (2004).

153. H. Adachi, Y. Hosokawa, K. Takano, F. Tsunesada, H. Masuhara, M. Yoshimura, Y. Mori, T. Sasaki. *J. Jpn. Assoc. Cryst. Growth (Japanese)* **29**, 35 (2002).
154. H. Adachi, K. Takano, Y. Hosokawa, T. Inoue, Y. Mori, H. Matsumura, M. Yoshimura, Y. Tsunaka, M. Morikawa, S. Kanaya, H. Masuhara, Y. Kai, T. Sasaki. *Jpn. J. Appl. Phys*. **42**, Part 2, L798 (2003).
155. H. Adachi, Y. Hosokawa, H. Masuhara, M. Yoshimura, Y. Mori, T. Sasaki. *Rev. Laser Eng. (Japanese)* **32**, 84 (2004).
156. Y. Hosokawa, H. Adachi, M. Yoshimura, Y. Mori, T. Sasaki, H. Masuhara. *Cryst. Growth Des.* **5**, 861 (2005).
157. H. Masuhara, S. Kawata (Eds.). *Nanoplasmonics: From Fundamental to Applications*, Elsevier, Amsterdam (2005).